Taylor & Francis
Taylor & Francis Group

ORIGINAL RESEARCH

🔓 OPEN ACCESS   ⓡ Check for updates

Low-dose CDK4/6 inhibitors induce presentation of pathway specific MHC ligands as potential targets for cancer immunotherapy

Angel Charles[a,#], Christopher M. Bourne ⓘ[b*,#], Tanya Korontsvit[a], Zita E. H. Aretz[c], Sung Soo Mun[a], Tao Dao[a], Martin G. Klatt[a*], and David A. Scheinberg[a,d*]

[a]Molecular Pharmacology Program, Sloan Kettering Institute, New York, USA; [b]Immunology and Microbial Pathogenesis Program, Weill Cornell Medicine, New York, USA; [c]Physiology, Biophysics and Systems Biology, Weill Cornell Medicine, New York, USA; [d]Pharmacology Program, Weill Cornell Medicine, New York, USA

ABSTRACT
Cyclin dependent kinase 4/6 inhibitors (CDK4/6i) lead to cell-cycle arrest but also trigger T cell-mediated immunity, which might be mediated by changes in human leukocyte antigen (HLA) ligands. We investigated the effects of CDK4/6i, abemaciclib and palbociclib, on the immunopeptidome at nontoxic levels in breast cancer cell lines by biochemical identification of HLA ligands followed by network analyses. This treatment led to upregulation of HLA and revealed hundreds of induced HLA ligands in breast cancer cell lines. These new ligands were significantly enriched for peptides derived from proteins involved in the "G1/S phase transition of cell cycle" including HLA ligands from CDK4/6, Cyclin D1 and the 26S regulatory proteasomal subunit 4 (PSMC1). Interestingly, peptides from proteins targeted by abemaciclib and palbociclib, were predicted to be the most likely to induce a T cell response. In strong contrast, peptides induced by solely one of the drugs had a lower T cell recognition score compared to the DMSO control suggesting that the observed effect is class dependent. This general hypothesis was exemplified by a peptide from PSMC1 which was among the HLA ligands with highest prediction scores and which elicited a T cell response in healthy donors. Overall, these data demonstrate that CDK4/6i treatment gives rise to drug-induced HLA ligands from G1/S phase transition, that have the highest chance for being recognized by T cells, thus providing evidence that inhibition of a distinct cellular process leads to increased presentation of the involved proteins that may be targeted by immunotherapeutic agents.

.Introduction

The development of targeted cancer therapies is an important and challenging part of cancer therapy, as traditional antineoplastic agents (e.g. chemotherapy, radiation) are nonspecific, and prone to off-target toxicities to healthy tissues and escape of cancer cells.[1,2] Other successful therapies such as immune checkpoint blockade and adoptive T-cell therapy target cancer-associated antigens,[3,4] but are generally nonspecific immune activators often associated with severe toxicities. Checkpoint blockade therapies rely on the ability of T-cells to recognize and kill cancer cells that express cognate HLA/peptide complexes presenting new antigens.[5,6]

Mutated neoantigens as HLA ligands provide ideal cancer specificity, but are patient-specific.[7] Therefore, more broadly expressed tumor-selective targets are needed to develop more widely applicable immunotherapies. T-cell receptor (TCR)-based therapies, including adoptive T cells and checkpoint blockade inhibitor antibodies, can target intracellular cancer-associated proteins if these are presented as peptides on the cell surface, thus making most proteins in the cell potential targets.[8,9] This key feature of TCR surveillance can be exploited to target intracellular, oncogenic and tumor selective pathways.

Previous studies have shown that drugs interfering with oncogenic signaling pathways can lead to the presentation of HLA ligands on cancer cells that are usually not displayed in healthy tissues,[10,11] offering the potential for immunotherapuetic targeting. For example, inhibition of the mitogen-activated protein kinase (MAPK) pathway in MAPK-driven cancers leads to improved peptide/MHC target recognition and killing by T cells and TCR-mimic antibodies.[10] Additionally, the inhibition of two tyrosine kinases, anaplastic lymphoma kinase (ALK), and rearranged during transfection (RET), in the cancers in which these pathways are oncogenic, promotes HLA class I antigen presentation, and induces expression of new peptides that are recognized by T cells.[11]

Despite rapid advancements in the treatment of breast cancer, many patients still relapse and are not cured. T cell-based immunotherapy strategies for breast cancer have been largely unsuccessful.[12] Therefore, discovery of therapeutic strategies that would increase susceptibility of breast cancer to immunotherapies is an attractive goal. Cyclin dependent kinase 4/6 inhibitors (CDK4/6i), which prevent the transition from G1 to the S phase of the cell cycle, have been shown to increase the expression of HLA class I molecules in multiple breast cancer cells lines.[13,14] CDK4/6i treatment has also been demonstrated to improve T cell infiltration into the tumor, and to work synergistically with immune checkpoint blockade (e.g. PD-L1) in mouse models.[13]

We hypothesized that CDK4/6 inhibitors could lead to presentation of new, drug-induced cancer-associated antigens that might be used for immunotherapeutic targeting and indeed, reports from single proteins of the CDK4/6 axis, such as cyclin D1 have been detected in melanoma after CDK4/6i treatment.[15] Utilizing HLA-peptide immunoprecipitation in conjunction with mass spectrometry (MS), we identified the presentation of many new HLA ligands derived from proteins involved in G1/S phase of cell cycle transition, the phase in which cells are usually arrested when treated with CDK4/6i. Many of these drug-induced HLA ligands had not been identified in healthy tissues, which renders them appealing targets for immune checkpoint blockade, TCR-based therapies and TCRmimic antibodies.[9] Additionally, we demonstrated reactivity of one of the induced HLA ligands with T cells from healthy donors. In summary, this concept illustrates drug-induced alteration of the immunopeptidome by CDK4/6i and also how disruption of G1/S phase transition of the mitotic cell cycle through small molecules can lead to increased presentation of proteins involved in that pathway. In this way, CDK4/6 inhibitors could potentially synergize with immunotherapuetic agents which target cell-cycle derived peptide-HLA complexes.

Results

Low-dose treatment with CDK4/6i increase HLA class I surface expression in breast cancer cells

MCF7 and T47D breast cancer cell lines were treated with either CDK4/6i abemaciclib or palbociclib to determine the lowest dose of CDK4/6i that would upregulate cell surface HLA expression, as this effect has been reported in the literature.[13] The MCF-7 cell line was chosen as positive control to repeat the published results. T47D cells were added as they also are known to be susceptible to CDK4/6i, but furthermore show higher HLA expression which made them a better candidate for an HLA ligand focused study. Drug concentrations of either abemaciclib or palbociclib ranging from 10 to 1,000 nM, were applied over 7 days on MCF7. Flow cytometric analysis showed 100 nM as the lowest dose in which cell surface HLA levels were significantly upregulated, with abemaciclib inducing higher expression for MCF7 (Supplementary Fig. S1A). 100 nM of each drug was also tested on T47D and both similarly upregulated HLA, so palbociclib was chosen for further study to demonstrate the effects of another CDK4/6i on a different breast cancer cell line (Supplementary Fig. S1B). Importantly, 100 nM of either drug was about 100-fold lower than the respective IC50 values (about 10uM) for the cytostatic effect mediated by these drugs (Supplementary Fig. S1B, S1C), and 2–3 fold lower than plasma concentrations in patients treated with these drugs.[16] Therefore, observed effects were unlikely to be associated with the cytostasis of these cells. By bright field microscopy and flow cytometry, the 100 nM dose of Abemaciclib resulted in an increase in MCF7 cell size when compared to DMSO treatment (Figure 1a, Supplementary Fig. S1D); at the same time point, T47D cells also showed an increase in overall cell size, taking on a more spherical morphology and increase in granularity when compared to DMSO treated cells (Figure 1b, Supplementary Fig. S1E).

A 7 day time-course experiment with low-dose (100 nM) abemaciclib treatment resulted in a doubling of HLA-A*02 and pan-HLA class I surface expression per cell (Figure 1a, left and
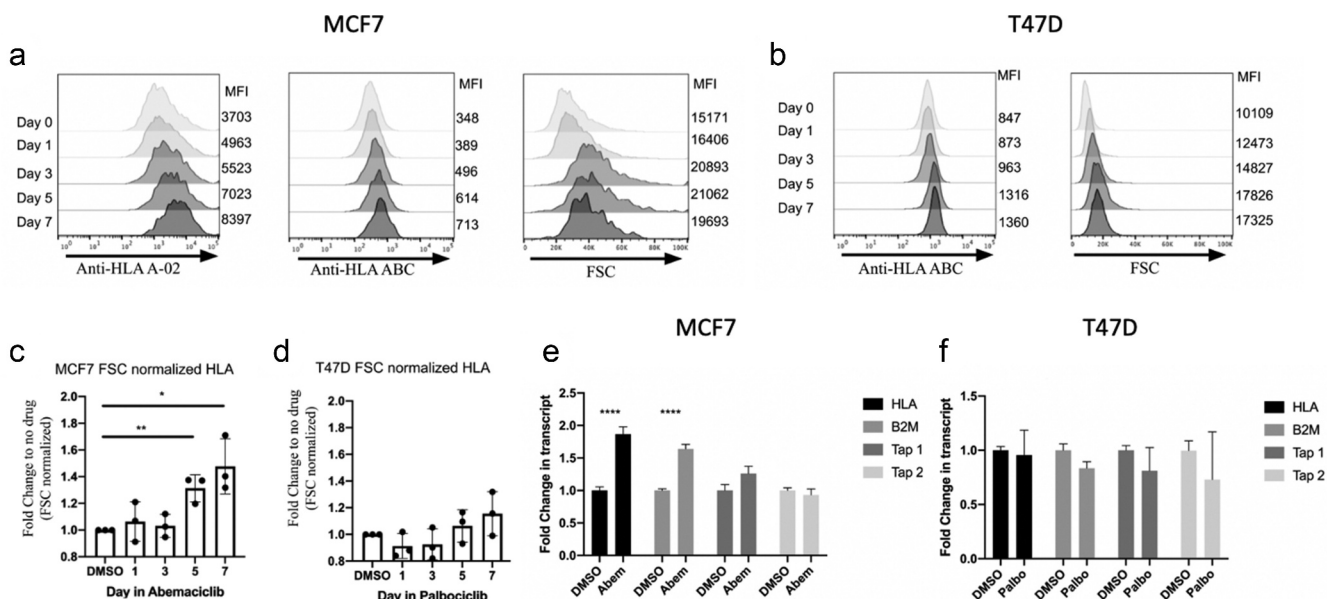
Figure 1. CDK4/6 inhibitors increase HLA surface expression. (a) MCF7 breast cancer cells were treated with 100 nMabemaciclib for the amount of time indicated on the Y axis. Flow cytometry for HLA-A02 levels (left), pan HLA levels (middle), and forward scatter (right) are displayed against corresponding mean fluorescence intensity (MFI) in x axis and the level is annotated on the right side. (b) T47D breast cancer cells were treated with 100 nM palbociclib for indicated times using flow cytometry as in panel A. (c) Normalized fold change in MFI from panel A of three biological replicates. HLA expression was normalized to forward scatter (FSC) to account for cell size changes and expressed as fold change to DMSO. (d) Normalized fold change in MFI from panel B of three biological replicates. HLA expression was normalized to forward scatter (FSC) to account for cell size changes and expressed as fold change to DMSO. (e-f) qRT-PCR for key proteins involved in antigen presentation transcripts noted on insert legend was performed on (e) MCF7 cells and (f) T47D cells, 7 days after treatment with a single dose of 100 nM abemaciclib or palbociclib on day 1. Error bars indicate SD, *P < .05, ** P < .01, *** P < .001, **** P < .0001. All experiments were performed in technical replicates.

middle), as well as moderate increases in cell size in MCF7 breast cancer cells (Figure 1a, right). Similar effects were observed after treatment with 100 nM palbociclib in T47D cells (Figure 1b). However, when total pan-HLA class I surface expression was recalculated and normalized for the increase in cell size, the treatment showed a statistically significant 50% increase in pan-HLA class I surface expression *density* in MCF7 cells treated with abemaciclib compared to DMSO by day 5 (Figure 1c); in contrast, for T47D cells, little and non-significant increase in HLA class I surface *density* was observed (Figure 1d). These results suggest that HLA class I surface expression is increased independently of the increase in cell surface size in MCF7 cells but is largely mediated through increases in cell size in T47D cells, an effect that may not have been taken into consideration in previous studies.[13]

The increase in HLA class I surface expression that was seen with CDK4/6i treatment could be due to a number of factors including increased transcription or translation of proteins involved in HLA expression, increased stabilization of HLA molecules on the cell surface, [11] or increased peptide transport to the endoplasmic reticulum. In order to gain insight into the mechanism underlying the observed phenomena, we performed qRT-PCR analysis on key gene products involved in antigen presentation. In MCF7 cells treated with 100 nM of abemaciclib, there was a 1.5–2 fold increase in the transcript levels of both *hla* and *beta-2-microglobulin* (*b2M*), but little change in transcript levels of the *transporter associated with antigen processing 1 and 2* (*tap1* and *tap2*) proteins when compared to DMSO (Figure 1e). This is in contrast to previous

studies which did show an upregulation of TAP proteins for MCF-7, MDA-MB453 and patient derived cancer cells at higher treatment concentrations compared to the concentrations used in this study.[13] Moreover, in T47D cells treated with palbociclib, there were no significant changes in *hla*, *b2M*, or *tap1* transcript levels, when compared to DMSO (Figure 1f). These results imply that the increase in HLA class I surface protein levels observed in CDK4/6i treated breast cancer cells were not consistent with a broad upregulation in antigen presentation, which differs from previous observations which showed upregulation of various components of antigen presentation with CDK4/6 treatment.[13]

Mass spectrometry identified changes in the immunopeptidome after CDK4/6i treatment

To investigate how alterations in surface HLA levels affect the repertoire of presented HLA ligands, we biochemically isolated HLA class I (HLA-A, HLA-B and HLA-C) peptides from breast cancer cells treated with either abemaciclib, palbociclib, or DMSO, assigned them to their HLA alleles through the netMHCpan 4.0[17] prediction algorithm and mapped the peptides to their proteins of origin (Supplementary Table 1).

In the MCF7 cell line, CDK4/6i treatment increased the number of unique identified HLA ligands 1.5 or 1.9-fold for palbociclib or abemaciclib, respectively resulting in 160 or 200 unique HLA class I ligands (Figure 2a, b). Compared to DMSO, results from abemaciclib and palbociclib combined induced the presentation, in total, of more than 200 new HLA class
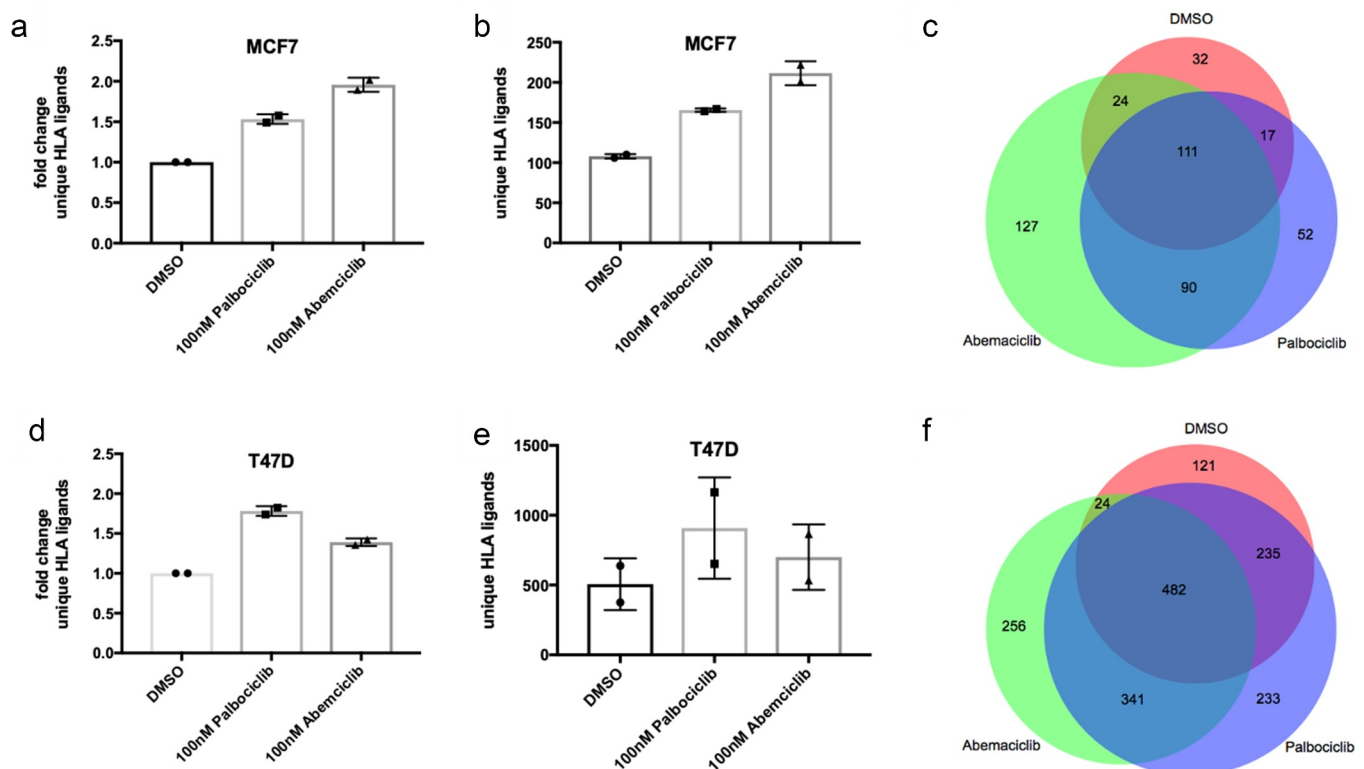
Figure 2. CDK4/6i induce changes in the immunopeptidome of breast cancer cells. Immunoprecipitation of HLA complexes and subsequent isolation and analysis of HLA-bound peptides by LC-MS/MS was performed after 7 day treatment with either 100 nM DMSO, Abemaciclib or Palbociclib. MCF and T47D cells respectively, showed relative (a,d) and absolute increases in unique HLA ligands (b, e) after drug treatment compared to DMSO treatment. Venn diagrams for MCF7 (c) and T47D (f) illustrate induction of HLA ligands. Error bars indicate mean and SD of two biological replicates.

I ligands at concentrations of 100 nM of either drug (Figure 2c). In the T47D cell line much higher total numbers of HLA ligands were detected, consistent with previously published data that determined that absolute HLA transcript levels are almost 3-fold higher in T47D compared to MCF7 cells.[18] An average of 908 and 700 unique HLA ligands were identified in the palbociclib and abemaciclib treated cell lines respectively, compared to 506 in DMSO treated cells. The relative increase was about 1.7 and 1.4-fold, respectively (Figure 2d, e). This resulted in a total of more than 500 new HLA class I ligands induced by either drug CDK4/6i treatment (Figure 2f), demonstrating that though the increase in total HLA surface levels was highly influenced by the increase in cell size for T47D cells, the overall immunopeptidome still expanded notably. Although overall antigen presentation is not affected by CDK4/6i in this cell line, increased HLA surface area and changes to cellular states are sufficient to modulate the immunopeptidome. Of note, the numbers of identified HLA ligands matched or exceeded the amount of ligands recently reported on the same breast cancer cell lines[18] and are in line with the relative amounts of HLA complex presented on their cell surface.[19] The results showed a trend for the upregulation of HLA ligands (p = .09). While not at $p < .05$, the narrow distribution of the error bars support the validity of the findings.

Interestingly, further analysis of the HLA ligands showed that the increase in HLA ligand presentation changed neither the HLA allelic association (Supplementary Fig. S2A, S2B), nor the length distribution of the HLA ligands (Supplementary Fig. S2C, S2D) ensuring consistency of the approach and excluding potential bias through different processing after drug treatment.

CDK4/6i-induced HLA ligands are derived from proteins enriched in G1/S cell cycle transition

To further understand if there was a correlation between the inhibition of the CDK4/6 complex and the change in the immunopeptidome, we analyzed the source proteins of the drug-induced HLA ligands. Results from biological replicates of the different treatment conditions were combined for every cell line individually and source proteins lists were generated from either all proteins in the DMSO samples or from all source proteins induced from CDK4/6i treatment (Figure 3 A, B, left panel, Supplementary Table 2). The network analysis was performed using GeneMANIA[20] and focused on physical interactions rather than co-expression or genetic interactions, to address the direct physical inhibition of the CDK4/6 complex and pathways by this drug class. Network analyses clearly demonstrated a strong enrichment for proteins from the G1/S transition of cell cycle (q values of $2.5*10^{-6}$ for MCF7 and $8.8*10^{-19}$ for T47D cells). The enrichment of this class of proteins was the top hit for both cell lines after drug treatment, and specifically not enriched in the cells after DMSO-treatment, suggesting a drug-specific effect that is consistent with the known mechanism of CDK4/6i leading to cell cycle arrest in G1 phase (Figure 3 A, B, right panel). Building a network of all the proteins identified in our study through CDK4/6i induction that are involved in the "G1/S transition of mitotic cell cycle" illustrated three subgroups relevant to the
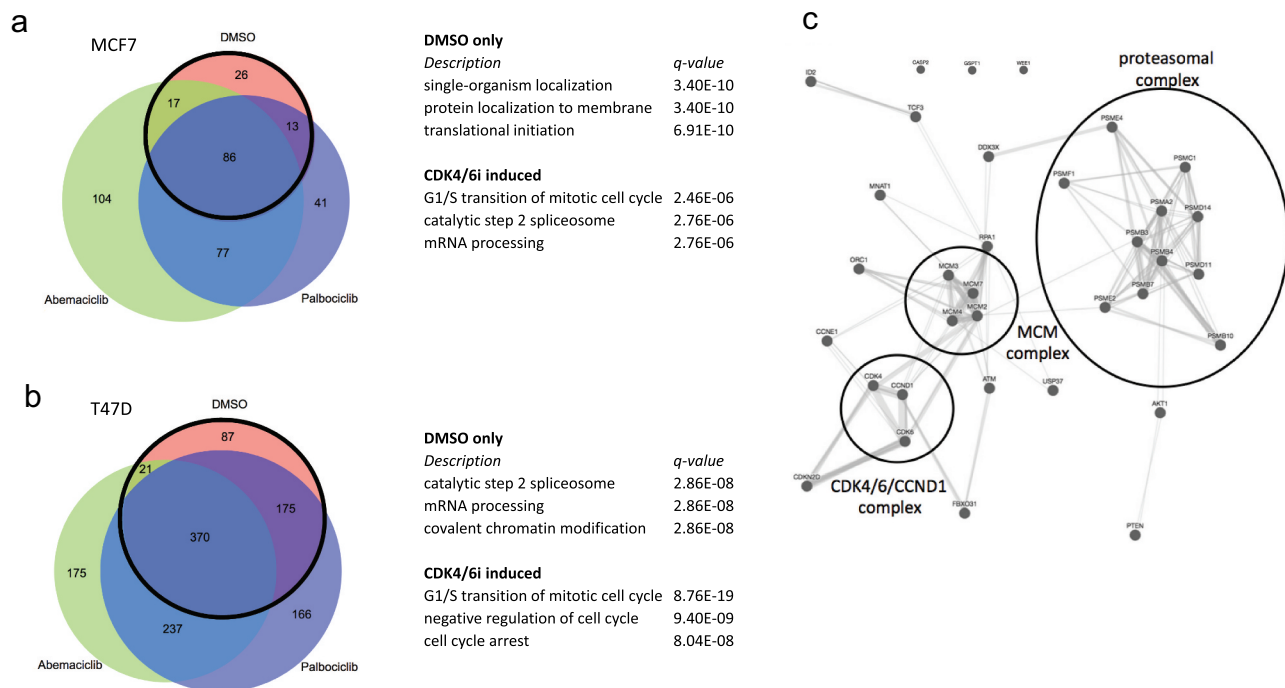
Figure 3. CDK4/6i induce MHC ligands enriched from source proteins contributing to "G1/S transition of mitotic cell cycle". Source proteins from peptide sequences detected either in the DMSO sample (inside the bold lined circle) or source proteins from CDK4/6i induced peptides (outside the bold lined circle) were used for network analyses. GeneMANIA was used for analysis and only physical interactions were enabled. Top 3 enriched GO terms are shown for MCF7 cells (a) and T47D cells (b). (c) Network analysis of physical interactions from all proteins induced by CDK4/6i treatment contributing to the GO term "G1/S transition of mitotic cell cycle". Circles indicate 3 clusters consisting of CDK4/CDK6/CCND1 complex (bottom left), MCM complex (middle) and proteasomal complex (upper right).

process: the CDK4/6/CCND1-complex (Figure 3c, lower left circle), the mcm-complex (Figure 3c, middle circle) and the proteasome (Figure 3c, upper right circle). Overall, a total of 60 unique HLA ligands (where post-translationally modified peptides are considered distinct from the unmodified counterpart) from various alleles and both cell lines were exclusively detected after drug treatment. These peptides were all derived from proteins from the G1/S cell cycle interactome. (Table 1). Of note, HLA ligands were repeatedly identified from the directly inhibited molecules CDK4 and CDK6, from the main interacting partner CCND1, and also from more distant physical interactors in the G1/S transition pathway, e.g. components of the mcm-complex. Other important proteins specifically induced after CDK4/6i treatment included the prognosis relevant proteins cyclin E1 (CCNE1) and many of the induced HLA ligands were derived from proteins that have not been reported to contribute to the immunopeptidome of

healthy tissues.[21] Notably, such cell cycle HLA ligands were induced in the T47D cell line at least equally well compared to MCF7 cells, even though T47D showed no evidence of increased antigen presentation machinery when normalized to cell size (Figure 1–2). This demonstrates that such an effect is independent and more robust between cell lines than changes in antigen presenting machinery.

Increased degradation of pathway specific source proteins as potential mechanism for increased presentation as HLA ligands

In order to better understand the mechanism underlying the induction of so many HLA ligands derived from the inhibited pathway, we focused on CCND1 as an important target as it is important for carcinogenesis in many cancer types[22,23] and proven to lead to immunogenic HLA ligands.[24,25]

Table 1. CDK4/6i induced peptides derived from proteins contributing to the GO term G1/S transtion of mitotic cell cycle.

Gene name	MCF7_DMSO	MCF7_Abemaciclib	MCF7_Palbociclib	T47D_DMSO	T47D_Abemaciclib	T47D_Palbociclib
CDK4			ALTPVVVTL (A02:01)		NPHKRISAF (B14:02)	
CDK6		ALTSVVVTL (A02:01) GEGAYGKVF (B44:02)				HRVVHRDL (B14:02)
CCND1		ALLESSLRQA (A02:01)			DRVLRAML (B14:02)	DRVLRAML (B14:02)
AKT1						SRHPFLTAL (B14:02)
ATM					DVHRVLVAR (A33:01)	
CASP2						STDTVEHSL (C08:02)
CCNE1					DAHNIQTHR (A33:01)	DAHNIQTHR (A33:01)
CDKN3					DSQSRSVSR (A33:01) DSQSRSVsR (A33:01)	DSQSRSVSR (A33:01) DSQSRSVsR (A33:01)
CDKN2D					NRFGKTAL (B14:02)	NRFGKTAL (B14:02)
DDX3X					DAYSSFGSR (A33:01)	
FBXO31					DVYAKLLHR (A33:01)	
GSPT1					EAEPGGGSL (C08:02)	EAEPGGGSL (C08:02)
ID2		ALDSHPTIV (A02:01)				
MCM2			AEAHARIHL (B44:02)		EAHARIHLR (A33:01)	
MCM3					HAQSIGMNR (A33:01) HAQSIGmNR (A33:01) DRTAIHEVM (B14:02)	HAQSIGMNR (A33:01) HAQSIGmNR (A33:01)
MCM4			RLAEAHAKV (A02:01)		HSMALIHNR (A33:01) HSmALIHNR (A33:01) DMRKIGSSR (A33:01) DmRKIGSSR (A33:01)	HSMALIHNR (A33:01) HSmALIHNR (A33:01) DMRKIGSSR (A33:01) DmRKIGSSR (A33:01) KRLHREAL (B14:02)
MCM7	RLAQHITYV (A02:01)	RADSVGKLV (C05:01) RLAQHITYV (A02:01) KmQEHSDQV (A02:01)	RLAQHITYV (A02:01) KmQEHSDQV (A02:01)			GRYNPRRSL (B14:02) TYTSARTLL (B14:02) VRLAHREQV (B14:02)
MNAT1					SSDLPVAL (C08:02)	
ORC1					NRVSSRLGL (B14:02)	
PSMA2					NYVNGKTFL (B14:02)	
PSMB10					FRYQGHVGA (B14:02) DRFQPNMTL (B14:02) DRFQPNmTL (B14:02)	DRFQPNMTL (B14:02) DRFQPNmTL (B14:02)
PSMB3		GLATDVQTV (A02:01)				
PSMB4					NRFQIATV (B14:02) YADGESFL (C08:02)	YADGESFL (C08:02)
PSMB7						FRYQGYIGA (B14:02)
PSMC1		IIDDNHAIV (A02:01)			EHAPSIVFI (B14:02)	EHAPSIVFI (B14:02)
PSMD11					VEFQRAQSL (B14:02)	VEFQRAQSL (B14:02)
PSMD14			FVDDYTVRV (A02:01)			
PSME2		KVLERVNAV (A02:01)		YHIISSNL (B14:02)		
PSME4					TRVDGRKL (B14:02)	TRVDGRKL (B14:02)
PSMF1					NNKDLYVLR (A33:01)	
PTEN					DFYGEVRTR (A33:01)	
RPA1					VSDFGGRSL (B08:02)	VSDFGGRSL (B08:02)
TCF3		SLDTQPKKV (A02:01)				
USP37					NRLPRVLIL (B14:02)	NRLPRVLIL (B14:02) DDLKRATEL (B14:02)
WEE1					DIKPSNIFISR(A33:01) EVYAHAVL (B14:02)	DIKPSNIFISR (A33:01)

Underlined peptides were tested in ELISpot assays.

Furthermore, CCND1 is the direct interacting partner of CDK4/6.[26] We exclusively identified peptides derived from CCND1 after CDK4/6i treatment in both cell lines, (ALLESSLRQA in complex with HLA-A*02:01 on MCF7 cells and DRVLRAML in complex with B*14:02 on T47D cells). We first evaluated the transcript and protein expression levels of cyclin D1 in CDK4/6i treated cells compared to DMSO during a 7-day time course. As reported, [27,28] we observed compensatory upregulation of *cyclin D1* transcript levels in both MCF7 and T47D cells treated with CDK4/6i which increased with longer exposure to drug (Figure 4a, 4b). Western blot analysis of the protein expression levels of Cyclin D1 in both breast cancer cell lines largely paralleled that of transcript, demonstrate slight increase in total intracellular Cyclin D1 (Figure 4c). This indicated that at the protein level, increased Cyclin D1 expression correlated with the exclusive detection of Cyclin D1 derived peptides in CDK4/6i treated breast cancer cells (Figure 4a-c, Table 1), suggesting that inhibition of this pathway might lead to a compensatory increase in protein levels and antigen presentation.

Next, we sought to determine if increased Cyclin D1 presentation in cells treated with CDK4/6i could be attributed to an increase in protein degradation through the multi-ubiquitin pathway. We immunoprecipitated multi-ubiquitinated proteins and then performed a western blot for Cyclin D1 at different time points. Similarly to the results observed for overall protein levels the amount of ubiquitinated cyclin D1

increased in CDK4/6i treated MCF7 and T47D cells compared to DMSO in a time dependent manner as indicated by higher molecular weight bands at later time points (Figure 4d arrows). Taken together, these results support a model whereby CDK4/6i led to compensatory upregulation of cell cycle proteins, followed by their degradation and presentation on HLA (Figure 5).

Drug-induced HLA ligands elicit T cell responses in healthy donors and have higher probability for T cell recognition

Finally, to demonstrate that CDK4/6i-induced HLA ligands were capable of eliciting T cell reactivity, we selected 8 peptides that were predicted to bind HLA-A*02:01 based on the netMHCpan4.0 algorithm including a CCND1- and CDK6-derived peptide. According to the T cell recognition score algorithm, [29] three of these eight peptides reached the threshold of 0.1, which suggests T cell recognition and reactivity; however, clear evidence of immunogenicity can only be given through T cell based functional assays. After T cell stimulation of four healthy donors with peptide-pulsed antigen presenting cells we repeatedly detected positive T cell responses by ELISpot for one of the three peptides predicted to have higher potential for reactivity and no responses for the remaining five peptides not being predicted to be immunogenic (Figure 4e, Table 2). The positive response was directed against IIDDNHAIV from PSMC1 protein, a cell cycle interactome
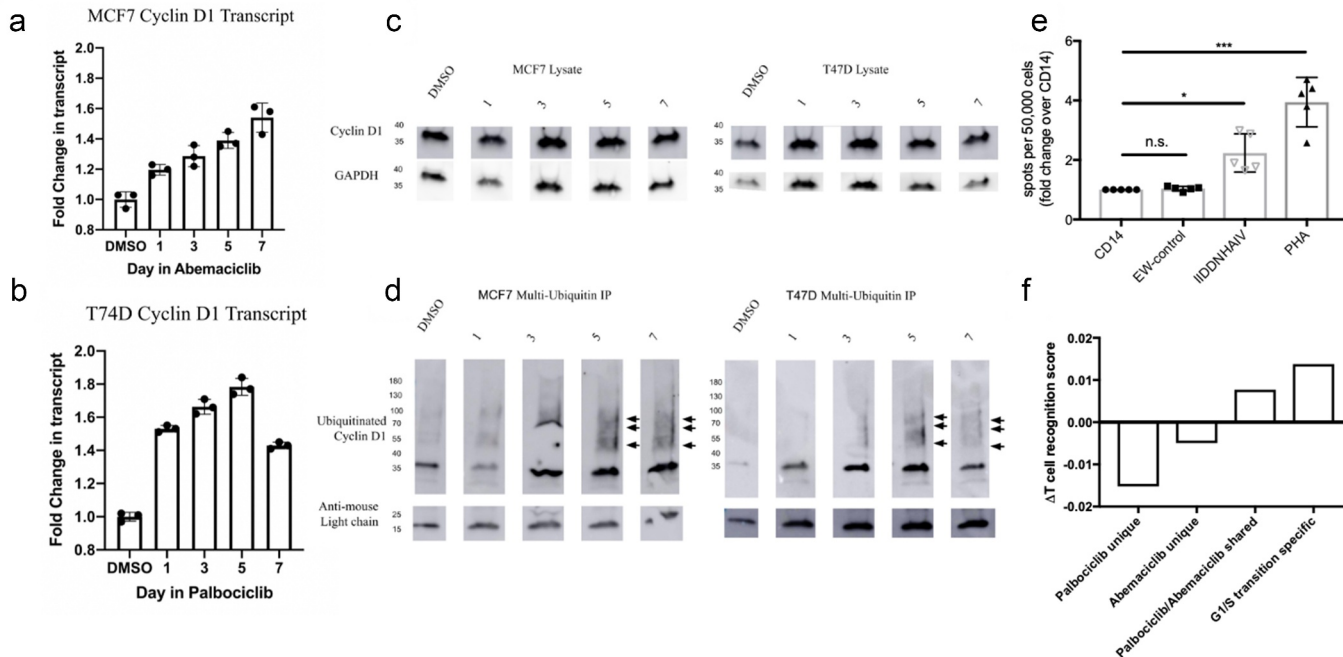
Figure 4. CDK4/6i alter cell cycle pathway for immunotherapeutic targeting. (a) MCF7 and (b) T47D breast cancer cells were treated with 100 nM abemaciclib or palbociclib, respectively, for indicated times. qRT-PCR of Cyclin D1 compared to Actin B was normalized to DMSO treated cells and technical replicates plotted. (c) Western blot for Cyclin D1 from lysates of MCF7 and T47D cells treated as described in (A) with times listed on top of each lane. Molecular weight is provided on the left axis (kD). (d) Ubiquitinated proteins were immunoprecipitated from cell lysates in (C), with times listed on top of each lane and Western blot was performed for Cyclin D1. Arrowheads denote higher molecular weight bands of Cyclin D1, indicative of increased ubiquitination. Molecular weight is provided on left axis (kD). Western blots were repeated twice with similar results. (e) ELISpot result from healthy donor's T cell stimulation with peptide loaded antigen presenting cells. CD14 positive cells and EW-peptide were used as negative control. PHA for positive control. Error bars indicate mean and SD of biological replicates. All data were normalized to the results of CD14 sample. Data are representative for 4 healthy donors and a total of 5 biological replicates. *$P < .05$, ** $P < .01$, *** $P < .001$, **** $P < .0001$ (f) T cell recognition predictions for HLA ligands from two different breast cancer cell lines using the iedb online platform[28] were performed. Graph shows the differences (delta) of mean T cell recognition values compared to predictions from HLA ligands found in DMSO-treated samples. Data represent the merged results from 2 different cell lines and all replicates.
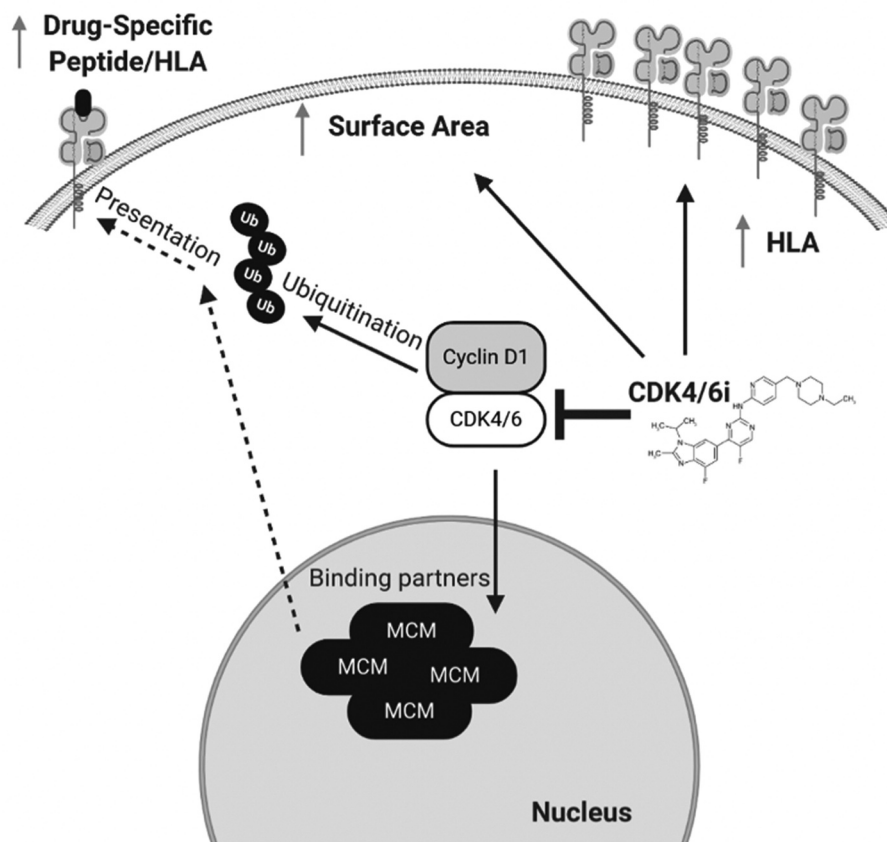
Figure 5. Proposed mechanism of increased CCND1 presentation after CDK4/6i treatment. CDK4/6i inhibit CDK4/6 and their binding partners, leading to ubiquitination. CDK4/6i also promotes compensatory upregulation of cell cycle proteins, HLA, and increased surface area. Together, these mechanisms lead to presentation of a wide variety of cancer-specific peptides derived from cell cycle effectors.

Table 2. Predictions and assays for T cell recognition in drug-induced A*02 ligands.

HLA ligand	Predicted binding affinity for HLA-A*02 [nM]	T cell recognition score	ELISpot result
ALLESSLRQA	414.5	−0.260	negative
ALTSVVVTL	35.8	−0.018	negative
FVDDYTVRV	6.8	0.130	negative
GLATDVQTV	23.5	0.037	negative
IIDDNHAIV	115.8	0.160	positive
KVLERVNAV	19.4	0.200	negative
RLAEAHAKV	16.2	0.089	negative
SLDTQPKKV	1878.4	−0.380	negative

protein that in a recent study was shown not to give rise to any HLA ligands in healthy tissues.[21] These published data support the idea of no preexisting tolerance against this peptide. However, as testing dozens of peptides for T cell recognition by T cell assays is cumbersome and potentially still biased by small numbers we performed T cell recognition predictions for all drug-induced peptides compared to DMSO-treated control cell lines using aforementioned algorithm[29] to determine tendencies for T cell reactivity within the different groups. We calculated the average of T cell recognition scores for peptides found in the DMSO-treated samples for each cell line separately to avoid bias introduced by different HLA types. Next, we calculated mean T cell recognition scores for different subsets of induced HLA ligands accordingly for each cell line separately but including all replicate data. Following subsets of HLA ligands were used: palbociclib unique, abemaciclib unique, shared between palbociclib and abemaciclib samples and HLA ligands from proteins involved in the G1/S phase transition GO term, called "G1/S transition specific" which correspond to the HLA ligands listed in Table 1. Finally the difference between mean T cell recognition scores from DMSO and aforementioned induced subsets was calculated per cell line and then results for both cell lines added. Intriguingly, mean T cell recognition scores from induced HLA ligands found exclusively either in the palbociclib or abemaciclib samples showed lower scores compared to the DMSO mean resulting in a negative T cell recognition score (Figure 4f). In contrast, HLA ligands shared between both drugs and especially HLA ligands derived from proteins involved in the biological process most effectively targeted by CDK4/6i (G1/S phase transition) were assigned higher T cell recognition scores compared to the DMSO group (Figure 4f) suggesting that HLA ligands specifically induced in a drug class-specific manner of CDK4/6i have the highest probability of being recognized by T cells. Furthermore, even if the absolute difference of the T cell recognition score between these subgroups is small the biological impact can be more profound as immune responses against few peptides can lead to relevant biological differences and T cell reactivity for one target has already been demonstrated after testing only eight candidates.

Discussion

Immunotherapies, such as immune checkpoint blockade therapy are now standard of care for many cancer types.[30] However, for many cancer types, checkpoint blockade remains unsuccessful likely due to lack of presentation of suitable immunogenic epitopes, e.g. neoepitopes or tumor associated antigens on the cancer cell surface.[31,32] Similarly, adoptive T cell therapies, ImmTacs, vaccines, or TCRmimic antibodies also depend on the reliable presentation of the HLA ligand for which they are specific, on the target cells.[7,9,33,34]

CDK4/6 inhibitors, abemaciclib and palbociclib, led to an increase in total surface area of treated breast cancer cells, as well as transcriptional upregulation of HLA in the MCF7 cell line. Although increases in HLA may be due in part to the enlarged cell volume in the T47D cell line, we still observed quantitative and qualitative changes in the immunopeptidome by mass spectrometry in both the MCF7 and T47D cell lines. These results indicated that an increase in HLA complex levels may broaden the repertoire of detectable presented antigens even when higher HLA cell surface levels are due in part to an expanded cell surface area and not to an increase in antigen presentation. Though increasing cell size and granularity could suggest senescence related mechanisms for the observed effect we believe that these cells did not present a strong senescence phenotype as determined by negative staining for the newly identified senescence marker urokinase plasminogen activator receptor ([35], data not shown).

Additionally, in contrast to previous results, we did not observe significant changes in transcription of antigen presentation machinery, as a whole [13] This could be explained by the 3–5 times lower concentration of CDK4/6i that was used in our study compared to previous published work.

Lower doses of drug were further used in our experiments to avoid confounding biochemical changes in the cell as a result of toxicity or cell death processes. The exact mechanism of HLA upregulation and induction of antigen presentation by this class of inhibitors is still unknown. These results suggest that CDK4/6i has indirect effects on increased HLA surface expression, and a transcriptional program of antigen presentation does not seem to be induced, per se. Additionally, other studies showed induction of the immunopeptidome after treatment of MCF7 cells with abemaciclib.[14] As we also saw peptides derived from the immuno-proteasome subunit PSMB10 presented on the cell surface after CDK4/6i treatment, we provided further evidence of the activation of the immunoproteasome that would then also contribute to the re-shaping of the immunopeptidome. Also, we hypothesize that the presentation of peptides from proteasomal proteins is mediated by their regular degradation after upregulation of this set of proteins. The upregulation of the proteasome components is needed as the CDK4/6 inhibition leaves many proteins from the inhibited pathway without function and subject to degradation. As insufficient proteasomal activity then can lead to autophagy[25] proteasomal proteins are upregulated to guarantee the sufficient degradation.

However, most importantly, many of the drug-induced antigens we found on the CDK4/6i treated groups were associated with proteins from the mitotic pathways, specifically the

G1/S phase transition, the phase in which cells arrest after CDK4/6i treatment.[26] This suggested that inhibition of the cellular process by the drugs led to preferential degradation of proteins and subsequent presentation on HLA peptides from proteins in the cell cycle pathway interactome. CDK4/6i gave rise to about 70 induced HLA ligands from the specific GO term "G1/S transition of mitotic cycle", which represented about 10% of all treatment induced HLA ligands. Mass spectrometry analysis revealed the peptides "ALLESSLRQA" and "DRLVRAML," an HLA-A*02:01-presented and HLA-B*14 :02-presented peptide, respectively from the Cyclin D1 protein, among other peptides. In a previous study, the ALLESSLRQA sequence was predicted to be an HLA-A*02:01 binder, but had never been validated for its immunogenicity as it was considered a suboptimal HLA binder.[23] By using Quantitative Reverse Transcriptase-PCR and Western blotting analysis we confirmed a compensatory upregulation of CDK4/6 binding partners, such as Cyclin D1, after CDK4/6i treatment. Additionally, Cyclin D1 exhibited higher levels of ubiquitination in CDK4/6i treated cells. Taken together, we propose a mechanism of increased immunopeptidome repertoire after CDK4/6i treatment whereby disruption of the CDK4/CDK6/CCND1 complex leads to upregulation and subsequent degradation and presentation of cell cycle proteins (Figure 5). Though changes in the immunopeptidome due to CDK4/6i treatment have recently been reported in melanoma cell lines after CDK4/6i treatment[15] this is the first study to demonstrate pathway-dependent degradation and presentation of a directly inhibited protein complex and its downstream interacting partners. However, for future studies it should also be considered that CDK4/6i could lead to the induction of HLA ligands from non-coding regions as these drugs can induce expression of endogenous retroviral elements. Additionally, neoepitopes from germline or somatic mutations could also demonstrate a valuable source for HLA ligands with and without CDK4/6i treatment.

Furthermore, it still has to be determined if these effects can only be observed in cell lines fully dependent on the CDK4/6 pathway as CDK4/6 independent cell lines have not been used in this study. This is especially important as less CDK4/6-dependent cell lines are more likely to be treated with immune checkpoint inhibition in which our proposed mechanism can be particularly relevant. Also triple negative breast cancers should further be investigated for this mechanism as their cyclin E amplification allows them to bypass the CDK4/6 inhibition, but could still be subject to changes in the HLA ligandome, which then could be utilized therapeutically.

Still, many of these drug-induced HLA ligands offer the potential to be ideal targets for cancer immunotherapies. For example CCND1 is expressed in multiple cancers, e.g. mantle cell lymphoma[23] and native immunogenic peptides from this protein have been shown to induce CD4 and CD8+ cytotoxic T cell responses in HLA matched donors.[24,25] Therefore, Cyclin D1 targeted immunotherapies may synergize with CDK4/6 inhibition in a variety of cancer types. Additionally, CCNE1 is a known negative prognostic marker in breast cancer[36] and an extensive study of HLA ligands in healthy tissues did not detect any peptides from CCNE1 presented on

the cell surface of nonmalignant cells.[21] Given these characteristics CCND1 as well as CCNE1, together with the other induced CDK4/6i induced proteins, those targets should be considered promising targets for immunotherapy approaches. Additionally, we stimulated T cells from healthy donors with a selection of drug-induced A*02 restricted peptides and identified an epitope from the PSMC1 antigen which elicited T cell responses. Additionally, to consider all induced HLA ligands we performed predictions for the T cell recognition of HLA ligands identified in DMSO-treated samples and for subsets of CDK4/6i-induced peptides. Strikingly, HLA-ligands found to be induced by both drugs rather than only one of them showed much higher T cell recognition scores as well as higher scores compared to the HLA ligands found in DMSO-treated cell lines. As HLA ligands that were induced by both drugs are more likely to be induced due to the class specific characteristics rather than off-target effects of these kinase inhibitors, this suggests that the specific targeting of the CDK4/6 complex leads to induction of HLA ligands of higher probability of T cell recognition. This hypothesis is further supported by the fact that HLA ligands from the GO term G1/S phase transition, the subset of peptides that are most likely to be induced by the class specific inhibition of these drugs, demonstrated even higher T cell recognition scores.

Overall, we demonstrated that low doses (100 nM) of CDK4/6 inhibitors abemaciclib and palbociclib can induce substantial and reproducible changes in HLA surface levels and in the ligands that are bound to these complexes, potentially rendering them more susceptible to immune mediated killing by CD8 + T cells. Considering that CDK4/6i have considerable toxicity (i.e. diarrhea, nausea, dyspnea, arthralgia, neutropenia and lymphopenia) at clinically used antineoplastic therapeutic doses.[37] Our results suggested that using concentrations 3 to 5-fold lower than patient plasma concentrations can still achieve significant drug-induced peptide presentation changes. However, *in vivo* studies have to be performed in order to investigate if low concentration CDK4/6i treatment can positively influence the effects of immune checkpoint blockade in breast cancer cells. If this can be proven, using lower doses of CDK4/6i at some appropriate time point may mitigate toxicity while synergizing with immunotherapies.

Additionally, we provide the proof-of-concept how physical inhibition of a protein complex leads to the enhanced presentation of HLA ligands directly involved or associated with this complex. This approach could be used to combine the direct inhibition of a complex with a T cell immunotherapy-based approach that targets the specific degradation product of one of the proteins involved.

Therefore, this study provides additional evidence and rationale to combine low-dose CDK4/6i with immunotherapies, such as checkpoint blockade. More over, generating immunotherapeutics that can target cell-cycle derived peptides presented on HLA are attractive. For example adoptive T cell transfer, TCRmimic antibodies or vaccination therapies could allow for specific targeting of breast cancer cells in combination with CDK4/6i.

Materials and methods

Human cell lines

MCF7 (HLA-A*02:01, HLA-B*18:01, HLA-B*44:02, HLA-C*05:01) and T47D (HLA-A*33:01, HLA-B*14:02, HLA-C*08 :02) cell lines were cultured in RPMI medium (Gibco) supplemented with 10% FBS (Gibco), penicillin and streptomycin, and 1% L-glutamate. All cell lines were obtained from ATCC, and tested negative for mycoplasma. HLA typing was performed by American Red Cross.

Antibodies and commercial reagents

APC anti-Human HLA-A, B, C (clone W6/32) from Biolegend (Cat. No. 311409), FITC Anti-Human HLA-A2 from BD Biosciences (Cat. No. 551285), were used for flow cytometry. Unlabeled clone W6/32 antibody from BioXcell (Cat. No. BE0079), was used for HLA class I/peptide immunoprecipitation for mass spectrometry. Anti-Human Cyclin D1 (ab134175) from Abcam, and anti-multi ubiquitin magnetic beads from MBL International, were used for Western blot. All antibodies were kept at 4°C. Abemaciclib and Palbociclib were purchased from Sellekchem. The drugs were diluted to 10 mM stocks in DMSO, and kept at −20°C.

Viability assays

15,000 cells were cultured in 96 well plates with serial dilutions of abemaciclib and palbociclib. After 4 days, cells were resuspended in Cell Titer-Glo Luminescent Cell Viability Assay from Promega for 10 minutes, and agitated at room temperature. Luminescence in the 96 well plates was read using a microtiter plate luminometer (PerkinElmer).

Flow cytometry

Cells were treated with 10, 100, or 1000 nM abemaciclib or palbociclib for 1, 3, 5, or 7 days. Cells were harvested, washed with PBS, and labeled with 1:50 dilution of APC Anti-Human HLA-ABC and FITC Anti-Human HLA-A2 in buffer (2% FBS, 0.1% sodium azide, in PBS) for 30 minutes. Cells were analyzed using a Fortessa Flow Cytometer from BD Biosciences or a Guava flow cytometer from Millipore.

Quantitative reverse-transcriptase PCR

Cells were treated with 100 nM Abemaciclib or Palbociclib for 1, 3, 5, or 7 days. Cells were harvested, washed with PBS, and RNA was extracted using Qiagen RNA Easy Plus (Qiagen; #74134). cDNA was created using qScript cDNA SuperMix (Quantabio; #95048) according to recommended cycling times and temperatures in thermocycler. qPCR was performed using PerfeCTa FastMix II (Quantabio; #95118) and TaqMan real-time probes purchased from Life Technologies: HLA-A (Hs01058806_g1), beta-2-microglobulin (Hs00187842_m1), TAP1 (Hs00388677_m1), and TAP2 (Hs00241060_m1),

Cyclin D1 (Hs00765553_m1), GAPDH (Hs02758991), Actin B (Hs99999903_m1). Data were normalized to baseline expression of GAPDH or Actin B.

Immunopurification of HLA class I ligands

HLA class I ligands (HLA-A,B and -C) were isolated as described previously.[38] In brief, 40 mg of Cyanogen bromide-activated-Sepharose 4B (Sigma-Aldrich, cat. # C9142) were activated with 1 mmol/L hydrochloric acid (Sigma-Aldrich, cat. # 320331) for 30 minutes. Subsequently, 0.5 mg of W6/32 antibody (Bio X Cell, BE0079; RRID: AB_1107730) was coupled to sepharose in the presence of binding buffer (150 mmol/L sodium chloride, 50 mmol/L sodium bicarbonate, pH 8.3; sodium chloride: Sigma-Aldrich, cat. # S9888, sodium bicarbonate: SigmaAldrich, cat. #S6014) for at least 2 hours at room temperature. Sepharose was blocked for 1 hour with glycine (Sigma-Aldrich, cat. # 410225). Columns were was with PBS twice and equilibrated for 10 minutes. MCF7 and T47D breast cancer cells were treated with DMSO, 100 nmol/L Abemaciclib, or 100 nmol/L Palbociclib for seven days. Cells ($1x10^7 per condition$) were harvested with Cellstripper (Corning, cat. # 25–056-CI) and washed three times in ice-cold sterile PBS (Media preparation facility MSKCC). Afterward, cells were lysed in 1 mL 1% CHAPS (Sigma-Aldrich, cat. # C3023) in PBS, supplemented with 1 tablet of protease inhibitors (Complete, cat. # 11836145001) for 1 hour at 4°C. This lysate was spun down for 1 hour at 20,000 g at 4°C. Supernatant was run over the affinity column through peristaltic pumps at 1 mL/minute overnight at 4°C. Affinity columns were washed with PBS for 15 minutes, run dry, and HLA complexes subsequently eluted five times with 200 mL 1% trifluoracetic acid (TFA, Sigma/Aldrich, cat. # 02031). For the separation of HLA ligands from their HLA complexes, tC18 columns (Sep-Pak tC18 1 cc VacCartridge, 100 mg Sorbent per Cartridge, 37–55 mm Particle Size, Waters, cat. # WAT036820) were prewashed with 80% acetonitrile (ACN, Sigma-Aldrich, cat. # 34998) in 0.1% TFA and equilibrated with two washes of 0.1% TFA. Samples were loaded, washed again with 0.1% TFA, and eluted in 400 mL 30% ACN in 0.1%TFA followed by 400 mL 40% ACN in 0.1%TFA, then 400 mL 50% ACN in 0.1%TFA. Sample volume was reduced by vacuum centrifugation for mass spectrometry analysis.[11]

LC-MS/MS analysis of HLA ligands

Samples were analyzed by a high-resolution/high-accuracy LC-MS/MS (Lumos Fusion, Thermo Fisher). Peptides were desalted using ZipTips (Sigma Millipore; cat. #ZTC18S008) according to the manufacturer's instructions and concentrated using vacuum centrifugation prior to being separated using direct loading onto a packedin-emitter C18 column (75 mm ID/12 cm, 3 mm particles, Nikkyo Technos Co., Ltd). The gradient was delivered at 300 nL/minute increasing linear from 2% Buffer B (0.1% formic acid in 80% acetonitrile)/98% Buffer A (0.1% formic acid) to 30% Buffer B/70% Buffer A, over 70 minutes. MS and MS/MS were operated at resolutions of 60,000 and 30,000, respectively. Only charge states 1, 2, and 3 were allowed. 1.6 Th was chosen as the isolation window and the collision energy was set at 30%. For MS/MS, the maximum injection time was 100 ms with an AGC of 50,000.

Mass spectrometry data processing

Mass spectrometry data were processed using Byonic software (version 2.7.84, Protein Metrics) through a custom-built computer server equipped with 4 Intel Xeon E5-4620 8-core CPUs operating at 2.2 GHz, and 512 GB physical memory (Exxact Corporation). Mass accuracy for MS1 was set to 6 ppm and to 20 ppm for MS2, respectively. Digestion specificity was defined as unspecific and only precursors with charges 1, 2, and 3, and up to 2 kDa were allowed. Protein FDR was disabled to allow complete assessment of potential peptide identifications. Oxidization of methionine, N-terminal acetylation, phosphorylation of serine, threonine, and tyrosine were set as variable modifications for all samples. All samples were searched against the UniProt Human Reviewed Database (20,349 entries, http://www.uniprot.org, downloaded June 2017). Peptides were selected with a minimal log prob value of 2 corresponding to p-values<0.01 for PSM in the given database and were HLA assigned by netMHC 4.0 with a 2% rank cutoff. Similar processing was performed with Mascot and PEAKS algorithm on a model leukemia cell line BV173 as it yields higher numbers of HLA ligands. Byonic demonstrated an overlap of 79.3% with Mascot (PEAKS overlapped with Mascot by 76.9%) and 84.3% with PEAKS with the highest sensitivity observed for Byonic. In T47D cells DMSO, Abemaciclib and Palbociclib samples showed an overlap between Byonic and PEAKS of 75%, 67%, and 69%, respectively. For all T47D derived HLA ligands the identity between the two algorithms was 79% (Supplementary Figure 3).

Source proteins of identified HLA ligands were divided into proteins that were identified in DMSO samples and proteins only identified in drug-treated samples. These protein lists were used for network analyses using GENEmania online platform.[20] Only physical interactions were enabled and no resultant genes were allowed. Automatically selected weighting method was used and all terms with q-values <0.05 were considered significant.

Peptide stimulation and ELISpot assay

CD14+ monocytes were isolated from cell separation medium-purified (Fisher Scientific, Cat. Nr. 25072 Cl) PBMCs from HLA-A*02:01 healthy donors on Memorial Sloan Kettering Cancer Center (MSK) IRB-approved protocols by positive selection using mAb to human CD14 coupled with magnetic beads (Miltenyi Biotech, Cat. Nr. 130–050-201) and used for the first stimulation of T cells. The CD14- fraction of PBMCs was used for isolation of CD3 positive cells by negative immunomagnetic cell separation using a pan T cell isolation kit (Miltenyi Biotech, Cat. Nr. 130–096-535). The purity of the cells was regularly assessed in previous experiments and was always >98%. In vitro T cell stimulation and generation of monocyte-derived dendritic cells (DCs) from CD14+ cells was performed as previously described:[11] T cells were stimulated for 7 d in the presence of RPMI 1640 supplemented with 5% autologous plasma (AP), 20 ug/mL synthetic peptides, 1 ug/

mL B2-m, and 10 ng/mL IL-15. Monocyte-derived DCs were generated from $CD14^+$ cells, by culturing the cells in RPMI 1640 medium supplemented with 1% AP, 500 units/mL recombinant IL-4, and 1,000 units/mL GM-CSF. On days 2 and 4 of incubation, fresh medium with IL-4 and GM-CSF was either added or replaced half of the culture medium. On day 6, maturation cytokine cocktail was added. On day 7 or 8, T cells were re-stimulated with mature DCs, with IL-15. In most cases, T cells were stimulated three times in the same manner, using either DCs or $CD14^+$ cells as APCs. A week after final stimulation, the peptide-specific T cell response was examined by IFN-gamma enzyme-linked immunospot (ELISPOT) assay.

For the ELISpot assay HA-Multiscreen plates (Millipore) were coated with 100 uL of mouse anti-human IFN-gamma antibody (10 ug/mL; clone 1-D1K; Mabtech) in PBS, incubated overnight at 4°C, washed with PBS to remove unbound antibody, and blocked with RPMI 1640/10% autologous plasma (AP) for 2 h at 37°C. Purified $CD3^+$ T cells were plated with either autologous $CD14^+$ (10:1 E: APC ratio) or autologous DCs (30:1 E: APC ratio). Various test peptides were added to the wells at 20 ug/mL. Negative control wells contained APCs and T cells without peptides or with irrelevant peptides. Positive control wells contained T cells plus APCs plus 20 ug/mL phytohemagglutinin (PHA, Sigma). All conditions were done in triplicates. Microtiter plates were incubated for 20 h at 37°C and then extensively washed with PBS/0.05% Tween and 100 uL/well biotinylated detection antibody against human IFN-g (2 ug/mL; clone 7-B6–1; Mabtech) was added. Plates were incubated for an additional 2 h at 37°C and spot development was performed. Spot numbers were read and determined by Zellnet Consulting Inc.

Software and statistics

T cell recognition prediction were performed using an online tool found associated with iedb.[28] Only 9mer HLA ligands were considered as suggested by the inventors of the algorithm. For figure 4f mean T cell recognition scores from HLA ligands identified in the DMSO samples were calculated as baseline. Then mean T cell recognition scores were calculated for different subsets, e.g. Palbociclib unique, Palbociclib/Abemaciclib shared corresponding to Figure 2c and 2f or "G1/S phase specific" corresponding to Table 1. All calculations were initially made for each cell line separately to avoid confounding by different HLA types. Then, mean T cell recognition scores from above mentioned subsets were subtracted from DMSO baseline and results for both cell lines added to retrieve the final result. Figure 5 was created using Biorender.

Graphs except Venn diagrams were drawn with Graphpad Prism 7. For statistics built-in analyses from Graphpad Prism were used. Student's t test were used for qPCR and flow cytometry statistical analysis. Venn diagrams were prepared using the BioVenn online platform.[39] P values < .05 were considered significant.

ORCID

Christopher M. Bourne (iD) http://orcid.org/0000-0001-9290-4223

Author's Contributions

A.C., C.M.B. Z.E.H.A., S.S.M., T.K., and M.G.K., performed and analyzed experiments. M.G.K. and D.A.S. designed experiments. A.C., C.M.B., and M.G.K. wrote the original draft of the manuscript. T.D., M.G.K and D.A. S. supervised the project. D.A.S. provided funding and edited the manuscript. All authors reviewed and contributed to the manuscript.

Data availability

Mass spectrometry data have been deposited at the PRIDE archive with the dataset identifier PXD024965.

References

1. Fox P, Darley A, Furlong E, Miaskowski C, Patiraki E, Armes J, Ream E, Papadopoulou C, McCann L, Kearney N, et al. The assessment and management of chemotherapy-related toxicities in patients with breast cancer, colorectal cancer, and Hodgkin's and non-Hodgkin's lymphomas: a scoping review [Internet]. Eur J Oncol Nurs. 2017;26:63–82. doi:10.1016/j.ejon.2016.12.008.
2. Plummer C, Steingart RM, Jurczak W, Iakobishvili Z, Lyon AR, Plastaras JP, Minotti G. Treatment specific toxicities: hormones, antihormones, radiation therapy. Semin Oncol. 2019;46 (6):414–420. doi:10.1053/j.seminoncol.2019.01.006.
3. Sharpe AH, Pauken KE. The diverse functions of the PD1 inhibitory pathway [Internet]. Nat Rev Immunol. 2018;18(3):153–167. doi:10.1038/nri.2017.108.
4. Ribas A, Wolchok JD. Cancer immunotherapy using checkpoint blockade. Science. 2018;359:1350–1355.
5. Yin L, Dai S, Clayton G, Gao W, Wang Y, Kappler J, Marrack P. Recognition of self and altered self by T cells in autoimmunity and allergy. Protein Cell. 2013;4(1):8–16. doi:10.1007/s13238-012-2077-7.
6. Schumacher TN, Schreiber RD. Neoantigens in cancer immunotherapy. Science. 2015;348(6230):69–74. doi:10.1126/science.aaa4971.
7. Dubrovsky L, Dao T, Gejman RS, Brea EJ, Chang AY, Oh CY, Casey E, Pankov D, Scheinberg DA. T cell receptor mimic

antibodies for cancer therapy. Oncoimmunology. 2016;5(1): e1049803. doi:10.1080/2162402X.2015.1049803.

8. Chandran SS, Klebanoff CA. T cell receptor-based cancer immunotherapy: emerging efficacy and pathways of resistance. Immunol Rev. 2019;290:127–147. doi:10.1111/imr.12772.

9. Chang AY, Gejman RS, Brea EJ, Oh CY, Mathias MD, Pankov D, Casey E, Dao T, Scheinberg DA. Opportunities and challenges for TCR mimic antibodies in cancer therapy. Expert Opin Biol Ther. 2016;16(8):979–987. doi:10.1080/14712598.2016.1176138.

10. Brea EJ, Oh CY, Manchado E, Budhu S, Gejman RS, Mo G, Mondello P, Han JE, Jarvis CA, Ulmert D, et al. Kinase regulation of human MHC class I molecule expression on cancer cells. Cancer Immunol Res. 2016;4(11):936–947. doi:10.1158/2326-6066.CIR-16-0177.

11. Oh CY, Klatt MG, Bourne C, Dao T, Dacek MM, Brea EJ, Mun SS, Chang AY, Korontsvit T, Scheinberg DA, et al. ALK and RET inhibitors promote HLA class I antigen presentation and unmask new antigens within the tumor immunopeptidome. Cancer Immunol Res. 2019;7(12):1984–1997. doi:10.1158/2326-6066.CIR-19-0056.

12. Planes-Laine G, Rochigneux P, Bertucci F, Chrétien A-S, Viens P, Sabatier R, et al. PD-1/PD-L1 targeting in breast cancer: the first clinical evidences are emerging. a literature review. Cancers [Internet]. 2019;11:1033. doi:10.3390/cancers11071033.

13. Goel S, DeCristo MJ, Watt AC, BrinJones H, Sceneay J, Li BB, Khan N, Ubellacker JM, Xie S, Metzger-Filho O, Hoog J, et al. CDK4/6 inhibition triggers anti-tumour immunity. Nature. 2017;548(7668):471–475. doi:10.1038/nature23465.

14. Schaer DA, Beckmann RP, Dempsey JA, Huber L, Forest A, Amaladas N, Li Y, Wang YC, Rasmussen ER, Chin D, et al. The CDK4/6 inhibitor abemaciclib induces a T cell inflamed tumor microenvironment and enhances the efficacy of PD-L1 checkpoint blockade. Cell Rep. 2018;22(11):2978–2994. doi:10.1016/j.celrep.2018.02.053.

15. Stopfer LE, Mesfin JM, Joughin BA, Lauffenburger DA, White FM. Multiplexed relative and absolute quantitative immunopeptidomics reveals MHC I repertoire alterations induced by CDK4/6 inhibition. Nat Commun. 2020;11(1):2760. doi:10.1038/s41467-020-16588-9.

16. Pernas S, Tolaney SM, Winer EP, Goel S. CDK4/6 inhibition in breast cancer: current practice and future directions. Ther Adv Med Oncol. 2018;10:1758835918786451. doi:10.1177/1758835918786451.

17. Jurtz V, Paul S, Andreatta M, Marcatili P, Peters B, Nielsen M. NetMHCpan-4.0: improved peptide-MHC class I interaction predictions integrating eluted ligand and peptide binding affinity data. J Immunol. 2017;199(9):3360–3368. doi:10.4049/jimmunol.1700893.

18. Rozanov DV, Rozanov ND, Chiotti KE, Reddy A, Wilmarth PA, David LL, Cha SW, Woo S, Pevzner P, Bafna V, et al. MHC class I loaded ligands from breast cancer cell lines: a potential HLA-I-typed antigen collection. J Proteomics. 2018;176:13–23. doi:10.1016/j.jprot.2018.01.004.

19. Klatt MG, Aretz ZEH, Curcio M, Gejman RS, Jones HF, Scheinberg DA. An input-controlled model system for identification of MHC bound peptides enabling laboratory comparisons of immunopeptidome experiments. J Proteomics. 2020;228:103921. doi:10.1016/j.jprot.2020.103921.

20. Warde-Farley D, Donaldson SL, Comes O, Zuberi K, Badrawi R, Chao P, Franz M, Grouios C, Kazi F, Lopes CT, et al. The GeneMANIA prediction server: biological network integration for gene prioritization and predicting gene function. Nucleic Acids Res. 2010;38(Web Server issue):W214–20. doi:10.1093/nar/gkq537.

21. Marcu A, Bichmann L, Kuchenbecker L, Backert L, Kowalewski DJ, Freudenmann LK, et al. The HLA Ligand Atlas. A resource of natural HLA ligands presented on benign tissues [Internet].

bioRxiv. 2019. 778944. [cited 2020 Apr 18]. Available from: https://www.biorxiv.org/content/10.1101/778944v1

22. Chen J, Zurawski G, Zurawski S, Wang Z, Akagawa K, Oh S, Hideki U, Fay J, Banchereau J, Song W, Palucka AK, et al. A novel vaccine for mantle cell lymphoma based on targeting cyclin D1 to dendritic cells via CD40. J Hematol Oncol. 2015;8(1):35. doi:10.1186/s13045-015-0131-7.

23. Wang M, Sun L, Qian J, Han X, Zhang L, Lin P, Cai Z, Yi Q. Cyclin D1 as a universally expressed mantle cell lymphoma-associated tumor antigen for immunotherapy. Leukemia. 2009;23(7):1320–1328. doi:10.1038/leu.2009.19.

24. Von Bergwelt-baildon MS, Shimabukuro-Vornhagen A, Wendtner CM, Kondo E. Identification of native, immunogenic peptides from cyclin D1. Leukemia. 2010;24(1):209–211. doi:10.1038/leu.2009.184.

25. Dao T, Korontsvit T, Zakhaleva V, Haro K, Packin J, Scheinberg DA. Identification of a human cyclin D1-derived peptide that induces human cytotoxic CD4 T cells. Plos One. 2009;4(8):e6730. doi:10.1371/journal.pone.0006730.

26. Vijayaraghavan S, Karakas C, Doostan I, Chen X, Bui T, Yi M, Raghavendra AS, Zhao Y, Bashour SI, Ibrahim NK, et al. CDK4/6 and autophagy inhibitors synergistically induce senescence in Rb positive cytoplasmic cyclin E negative cancers. Nat Commun. 2017;8(1):15916. doi:10.1038/ncomms15916.

27. Scott SC, Lee SS, Abraham J. Mechanisms of therapeutic CDK4/6 inhibition in breast cancer. Semin Oncol. 2017;44:385–394. doi:10.1053/j.seminoncol.2018.01.006.

28. Chen SH, Gong X, Zhang Y, Van Horn RD, Yin T, Huber L, Burke TF, Manro J, Iversen PW, Wu W, et al. RAF inhibitor LY3009120 sensitizes RAS or BRAF mutant cancer to CDK4/6 inhibition by abemaciclib via superior inhibition of phospho-RB and suppression of cyclin D1. Oncogene. 2018;37(6):821–832. doi:10.1038/onc.2017.384.

29. Calis JJ, Maybeno M, Greenbaum JA, Weiskopf D, De Silva AD, Sette A, Keşmir C, Peters B. Properties of MHC class I presented peptides that enhance immunogenicity. PLoS Comput Biol. 2013;9(10):e1003266. doi:10.1371/journal.pcbi.1003266.

30. Vaddepally RK, Kharel P, Pandey R, Garje R, Chandra AB. Review of indications of FDA-approved immune checkpoint inhibitors per NCCN guidelines with the level of evidence. Cancers [Internet]. 2020;12(3):738. http://dx.doi.org/10.3390/cancers12030738

31. Gejman RS, Chang AY, Jones HF, DiKun K, Hakimi AA, Schietinger A, Scheinberg DA. Rejection of immunogenic tumor clones is limited by clonal fraction. Elife [Internet]. 2018;7. http://dx.doi.org/10.7554/eLife.41090 .

32. Wolf Y, Bartok O, Patkar S, Eli GB, Cohen S, Litchfield K, Levy R, Jiménez-Sánchez A, Trabish S, Lee JS, et al. UVB-induced tumor heterogeneity diminishes immune response in melanoma. Cell. 2019;179(1):219–35.e21. doi:10.1016/j.cell.2019.08.032.

33. Heemskerk B, Liu K, Dudley ME, Johnson LA, Kaiser A, Downey S, Zheng Z, Shelton TE, Matsuda K, Robbins PF, et al. Adoptive cell therapy for patients with melanoma, using tumor-infiltrating lymphocytes genetically engineered to secrete interleukin-2. Hum Gene Ther. 2008;19(5):496–510. doi:10.1089/hum.2007.0171.

34. Rafiq S, Purdon TJ, Daniyan AF, Koneru M, Dao T, Liu C, Scheinberg DA, Brentjens RJ. Optimized T-cell receptor-mimic chimeric antigen receptor T cells directed toward the intracellular Wilms Tumor 1 antigen. Leukemia. 2017;31(8):1788–1797. doi:10.1038/leu.2016.373.

35. Amor C, Feucht J, Leibold J, Ho YJ, Zhu C, Alonso-Curbelo D, Mansilla-Soto J, Boyer JA, Li X, Giavridis T, et al. Senolytic CAR T cells reverse senescence-associated pathologies. Nature. 2020;583(7814):127–132. doi:10.1038/s41586-020-2403-9.

36. Zhao Z-M, Yost SE, Hutchinson KE, Li SM, Yuan Y-C, Noorbakhsh J, Liu Z, Warden C, Johnson RM, Wu X, et al. CCNE1 amplification is associated with poor prognosis in patients with triple negative breast cancer. BMC Cancer. 2019;19(1):96. doi:10.1186/s12885-019-5290-4.

37. Choo JR-E, Lee S-C. CDK4-6 inhibitors in breast cancer: current status and future development. Expert Opin Drug Metab Toxicol. 2018;14:1123–1138. doi:10.1080/17425255.2018.1541347.

38. Klatt MG, Mack KN, Bai Y, Aretz ZE, Nathan LI, Mun SS, Dao T, Scheinberg DA. Solving an MHC allele specific bias in the reported immunopeptidome. JCI Insight. 2020. doi:10.1172/jci.insight.141264.

39. Hulsen T, De Vlieg J, Alkema W. Biovenn – a web application for the comparison and visualization of biological lists using area-proportional Venn diagrams. BMC Genomics. 2008;9(1):488. doi:10.1186/1471-2164-9-488.